



Tuning methyl 4,6-*O*-benzylidene α -D-glucopyranosides' gelation ability by minor group modifications

Marlon F. Abreu^a, Vítor T. Salvador^a, Letícia Vitorazi^a, Carlos E.N. Gatts^b, Denise R. dos Santos^b, Rosana Giacomini^b, Sergio L. Cardoso^b, Paulo C.M.L. Miranda^{a,*}

^a Institute of Chemistry, State University of Campinas, UNICAMP, Cidade Universitária Zeferino Vaz, Barão Geraldo, Campinas, P.O. Box: 6154, SP 13083-970, Brazil

^b Northern State University of Rio de Janeiro, UENF, Campos dos Goytacazes, RJ, Brazil

ARTICLE INFO

Article history:

Received 5 February 2012

Received in revised form 14 March 2012

Accepted 19 March 2012

Available online 3 April 2012

Keywords:

LMOG

SAFIN

Organogelators

Self-assembly

ABSTRACT

Ten methyl 4,6-*O*-benzylidene α -D-glucopyranosides were synthesized for the purpose of studying systematically the effect of small group changes at position 4 of the aromatic ring on the ability to gelate organic solvents. The gelation properties are discussed on the basis of small angle X-ray scattering (SAXS), Fourier transform infrared spectroscopy (FTIR), differential scanning calorimetry (DSC) measurements, and scanning electron microscopy (SEM) observations. Sol–gel transition temperatures were determined simultaneously by DSC and temperature-dependent FTIR measurements. The current study emphasizes that carbohydrates furnish not only valuable information about structural requirements for organogelator design, but also for molecular assembly systems in general.

© 2012 Elsevier Ltd. All rights reserved.

1. Introduction

Low molecular mass organogelators (LMOG) are an important class of functional compounds formed by small organic molecules (PM <3000) and are capable of creating a supramolecular structure with the ability to immobilize organic media, through anisotropic self-recognition and self-assembly.¹ The interaction among gelator monomers occurs through some functional groups that direct the initial stacking in the construction of self-assembled fibrillar networks. These aggregates can retain solvent molecules in nanopores of fibrillar networks through capillary effect.² Gels produced by organogelators differ from polymeric gels, whose tridimensional fibrous networks are formed by cross-linked covalent bonds. In organogelators, the aggregation is accomplished by physical interactions, that is, coulombic, hydrogen bonding, dipole–dipole, van der Waals, π – π stacking, hydrophobic interactions, or different combinations among them. Such types of non-covalent interactions guarantee a peculiar property for these systems: the thermoreversibility.³ Thermoreversible gelation has attracted the interest of diverse academic as well as industrial groups due to their potential applications as for example controlled drug delivery,⁴ chemical and physical molecular devices,⁵ synthesis of nanostructured templates,⁶ oil recovery,⁷ and paintings restoration.⁸ Understanding the supramolecular architecture of these gelators is an exciting and worthwhile challenge because despite their

diverse applicability, very little is known about their behavior and mechanism of gelation.⁹ So, it is hitherto unclear how to synthesize a new class of gelator and the most of them are discovered serendipitously.¹⁰ Several families of compounds with ability of organic media gelation have been reported, and examples include ureas,¹¹ steroids,¹² anthracenes,¹³ and monosaccharide derivatives.¹⁴ However, in order to improve gelation ability, it is important to synthesize and study the behavior of organogels to understand their unique properties more profoundly. To achieve this objective, intensive research has been focused on manipulating small changes in organogelator skeleton, focusing a refined knowledge about optimization of gelation properties, mainly strength and ability. In the case of 4,6-*O*-benzylidene- α -D-glucopyranosides,^{14a} anomeric carbon and the aromatic ring are the main sites for structure modification and study of gelation process. Insertions of groups such as nitro¹⁵ or amine¹⁶ at position 4 of the aromatic ring modify its electronic density and significantly alter the gelation ability. In this case, the electron withdrawing group (nitro) demonstrated the best gelation capacity in comparison to the amine group.¹⁷ However, variations both in the contribution of aromatic ring electronic density and chain size have not yet been explored simultaneously in order to evaluate van der Waals and π – π stacking contributions together. In this context, this work describes the synthesis of ten new glucose derivatives: five *n*-alkoxyl substituents (electron donating series) and five *n*-alkoxycarbonyl (electron withdrawing series) at position 4 of the aromatic ring. Additionally, gels formed by new organogelators were characterized by FTIR, SEM, DSC, and SAXS in order to study the role of these

* Corresponding author. Tel.: +55 19 35213083; fax: +55 19 35213023.

E-mail address: miranda@iqm.unicamp.br (P.C.M.L. Miranda).

substituents in the gelation process and to advance our knowledge of these systems.

2. Results and discussion

2.1. Synthesis of methyl

4,6-*O*-benzylidene- α -D-glucopyranoside derivatives

The glucose based gelators were synthesized by adapting methodologies well described in the literature with very slight modifications (Fig. 1). Firstly, *O*-methyl acetal was prepared in acidic medium to provide methyl α -D-glucopyranoside, **1**, where HCl was generated in situ by addition of few drops of thionyl chloride in anhydrous methanol. The synthesis of **1** was made selectively under the adopted conditions, that is, high temperature and long reaction time, and the desired isomer was easily obtained from the reaction media by crystallization.¹⁸ Alkylations of *p*-hydroxybenzaldehyde and *p*-formylbenzoic acid were carried out using the corresponding alkylation agents (*n*-alkyl bromide, n -C_nH_(2n+1)Br, where $n = 2, 3, 4, 8$, or 16 C) and resulted in the formation of products **2a–e** and **5a–e**.¹⁹ The respective dimethylacetals **3a–e** and **6a–e** were prepared by transacetalization reactions of **2a–e** and **5a–e** with trimethyl orthoformate in acidic medium.²⁰ Finally, the two series of gelators

4a–e and **7a–e** were obtained through a benzylidene acetal formation with OH groups at positions 4 and 6 of methyl α -D-glucopyranoside (**1**) in DMF.²¹ All compounds prepared were characterized by NMR, FTIR, and MS (see Section 4).

2.2. Gelation test of compounds **4a–e** and **7a–e**

Gelation tests were carried out using 13 organic solvents at different concentrations (between 10 and 150 mmol L^{−1}) for the gelators **4a–e** and **7a–e** (Table 1). Initially, the mixture was heated in a vial close to the solvent boiling point in an oil bath. The vial was kept inside the oil bath and was slowly cooled to room temperature, which took approximately 1 h. Next, the vial was gently agitated, inverted, and classified according to visual inspection. When the solution in the vial was immobilized without any flow after mechanical agitation, it was classified as a gel (G) as shown in Figure 2. Other classifications included: partial self-supporting precipitation (P_{ps}), when sample showed immobilization of the solvent similar to a gel, but mechanical agitation caused a visible separation of solid from the liquid phase; precipitation after cooling (P); soluble (S) and insoluble at high temperature (I).^{14a}

For all gels, the heating/cooling process could be repeated several times, indicating that these gels are completely thermorevers-

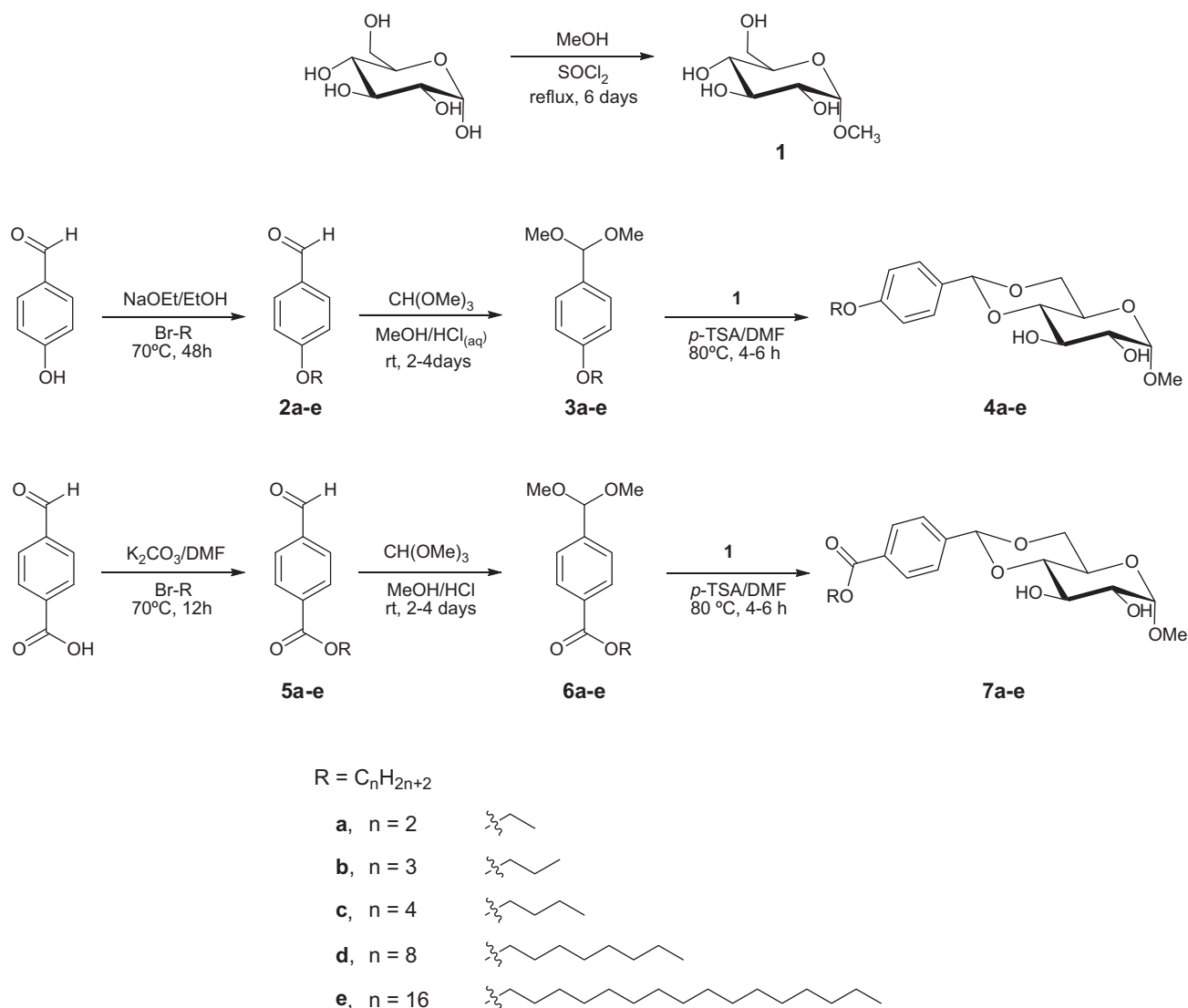


Figure 1. Synthesis of the LMOG of both series **4a–e** and **7a–e**.

Table 1Gelation test for compounds **4a–e** (*n*-alkoxyl substituents, the electron donating series) and **7a–e** (*n*-alkoxycarbonyl, the electron withdrawing series) in different organic solvents

Entry	Solvent	Electron donating series					Electron withdrawing series				
		4a	4b	4c	4d	4e	7a	7b	7c	7d	7e
		C ₂	C ₃	C ₄	C ₈	C ₁₆	C ₂	C ₃	C ₄	C ₈	C ₁₆
1	<i>n</i> -Heptane	I 10–150	I 10–150	I 10–150	G 10–30	G 10–100	I 10–150	I 10–150	I 10–150	G 10–60	G 10–150
2	Dodecane	G 15	G 15–20	G 15–20	G 10–40	G 10–110	I 10–150	G 15–20	G 10–120	G 10–150	G 10–150
3	<i>p</i> -Xylene	P _{ps} 10–20	G 15–90	G 15–120	G 15–120	G 15–150	P 60–150	G 15–100	G 10–150	G 10–150	G 10–150
4	Toluene	P _{ps} 20	G 20	G 20–90	G 20–80	G 20–150	I 10–150	G 10–50	G 10–150	G 20–150	G 10–150
5	Benzene	P 10–20	G 90	G 90–150	G 70–130	G 20–150	I 10–150	G 80–140	G 20–150	G 30–150	G 10–150
6	CCl ₄	I 10–150	I 10–150	G 20–150	G 30–150	G 20–150	I 10–150	I 10–150	G 20–150	G 20–150	G 10–150
7	C ₂ Cl ₄	P _{ps} 30	G 30	G 30–90	G 30–150	G 20–150	I 10–150	G 10–50	G 20–150	G 10–150	G 10–150
8	CH ₂ Cl ₂	S 10–150	S 10–150	S 10–150	S 10–150	S 10–150	S 10–70	S 10–150	S 10–150	S 10–150	S 10–150
9	Acetone	S 10–150	S 10–150	S 10–150	S 10–150	S 10–150	S 10–150	S 10–150	S 10–150	S 10–150	G 40–150
10	1-Butanol	P 30–150	G 120–150	G 110–150	G 100–150	G 30–150	P 60–150	G 110–150	G 80–150	G 80–150	G 30–150
11	1-Propanol	P 30–150	G 120–150	G 110–150	G 100–150	G 20–150	P 60–150	G 110–150	G 110–150	G 80–150	G 20–150
12	Methanol	S 10–150	S 10–150	S 10–150	G 130–150	G 20–150	S 10–150	S 10–150	S 10–150	G 130–150	G 20–150
13	DMSO	S 10–150	S 10–150	S 10–150	S 10–150	S 10–150	S 10–150	S 10–150	S 10–150	S 10–150	G 70–150

Concentration ranges are expressed in mmol L^{−1} below descriptors, which are (G) for gel formation after cooling without any flow after gentle mechanical perturbation; (P_{ps}) for solution immobilization after cooling, but with partial liquid flow after gentle mechanical perturbation; (P) for precipitation after cooling; (I) for insolubility at high temperature; and (S) for solubility at low temperatures.

ible. By analyzing Table 1, various inferences could be made for the characterization of gelation behavior of organogelators. In general, comparing the two series, *n*-alkoxycarbonyl derivatives (electron withdrawing series, **7a–e**) presented better gelation properties by immobilizing two more solvents than the other series: acetone and dimethylsulfoxide. Among 10 different compounds of both series, only **7a** was unable to form gel under the conditions studied. Another notable difference between these two groups was observed in the aforementioned concentration range. The other *n*-alkoxycarbonyl derivatives (electron withdrawing series, **7b–e**) formed gels in various solvents and at a wider range of concentrations than the electron rich series (**4a–e**). Interestingly, certain compounds of the electron deficient series (**7d–e**) gelled within the whole concentration range studied (10–150 mmol L^{−1}). In aprotic solvents with intermediate dielectric constant, that is, dichloromethane and acetone, all compounds but **7e** were soluble at room temperature. On the other side, protic polar solvents such as *n*-butanol and *n*-propanol were gelled by **4b–e** and **7b–e**, even methanol was gelled by compounds **4d–e** and **7d–e**. In the case of these solvents gelation took longer than 1 h, sometimes overnight

(methanol), and therefore suggestive of hydrogen bonding competition between gelator and solvent during the gelation process. Interestingly, compounds **4e** and **7e** revealed excellent gelation ability in comparison to the others, gelling from nonpolar to polar solvents. Between these two compounds, gelator **7e** was found to be the most efficient as it was capable of forming gel in a wider range of solvents and concentrations, even immobilizing acetone and dimethylsulfoxide as well. This characteristic is less common in most of gelators found in the literature, which gelate only a narrow range of solvents and concentration.^{14a,22} These results allowed to conclude that the presence of long alkyl chains in both series enhanced the ability to gelate various organic solvents. This may be possibly due to the contribution of van der Waals interaction and has been previously described for gelator methyl 4,6-O-benzylidene- α -D-glucopyranoside in the literature.^{14a} However, it should be noted that even gelators with shorter alkyl chains formed gels, although in a restricted range, and could be classified as good gelators. Finally, *n*-alkoxycarbonyl derivative series exhibited better gelation properties in comparison to the *n*-alkoxyl.

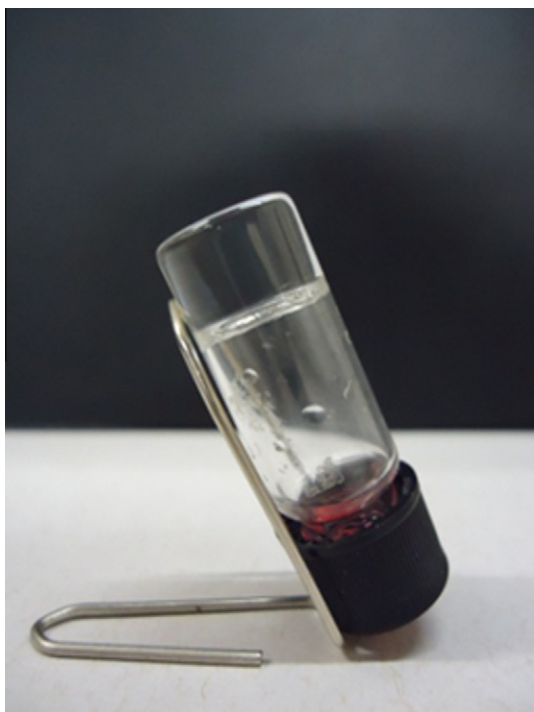


Figure 2. Photography of the organogel produced by compound **4e** in *p*-xylene at 30 mmol L⁻¹.

2.3. FTIR analyses

The FTIR spectroscopy with temperature variation was used to probe the intermolecular interactions among gelator molecules in both series (**4b–e** and **7b–e**) during gel formation. Several examples reported in the literature that use FTIR to characterize the primary interactions of the supramolecular structure of organogelators can

be found, principally for the molecules that can make hydrogen bonds.²³ However relatively few studies have investigated thermal evolution of samples during sol–gel transition.²⁴ In this work, experiments were conducted varying temperature from 50 °C to 30 °C for the purpose of being in close proximity to the sol–gel transition temperature in the chosen solvent (*p*-xylene). Initially, gels were prepared in *p*-xylene at a concentration of 30 mmol L⁻¹ for both series. Next, all samples were analyzed using FTIR coupled with a thermal system and the spectra in 3160–4000 cm⁻¹ region were acquired (Fig. 3). At the highest temperature (50 °C) all samples were found in sol phase and exhibited a peak at 3576 cm⁻¹, referring to the stretching vibration of the free OH group. Upon cooling the system to 30 °C, it is clearly observed that the OH peak broadens and substantially shifted toward a lower wavenumber (red-shift), indicating that organogelators aggregated and assembled themselves through hydrogen bonding. The 1640–1780 cm⁻¹ region (C=O stretching region) was also examined for compounds **7b–e**, but they had not revealed any significant difference among solutions and gels spectra. This behavior is the result of initial self-assembly of primary structure driven by the formation of a fibrous network. It is common to encounter these types of interactions in various derivatives of monosaccharide,^{14d} but in this work it was evidently predominant even with the increasing of the alkyl chain, which could favor van der Waals interactions in both these series. Nevertheless, we believe that the interaction among alkyl groups also contributed in the self-assembly of the secondary structure of fibrils as can be inferred from Table 1, where increase of the van der Waals force contribution augmented scope and rigidity of the gels.

2.4. Morphological study with SEM

The scanning electron microscopy (SEM)²⁵ was used for morphologic characterization of the supramolecular aggregate formed by gelators of the series **4b–e** and **7b–e** obtained from the xerogel in *p*-xylene. All these organogelators are aggregated in self-assembled fibrillar networks, which are responsible for the immobilization

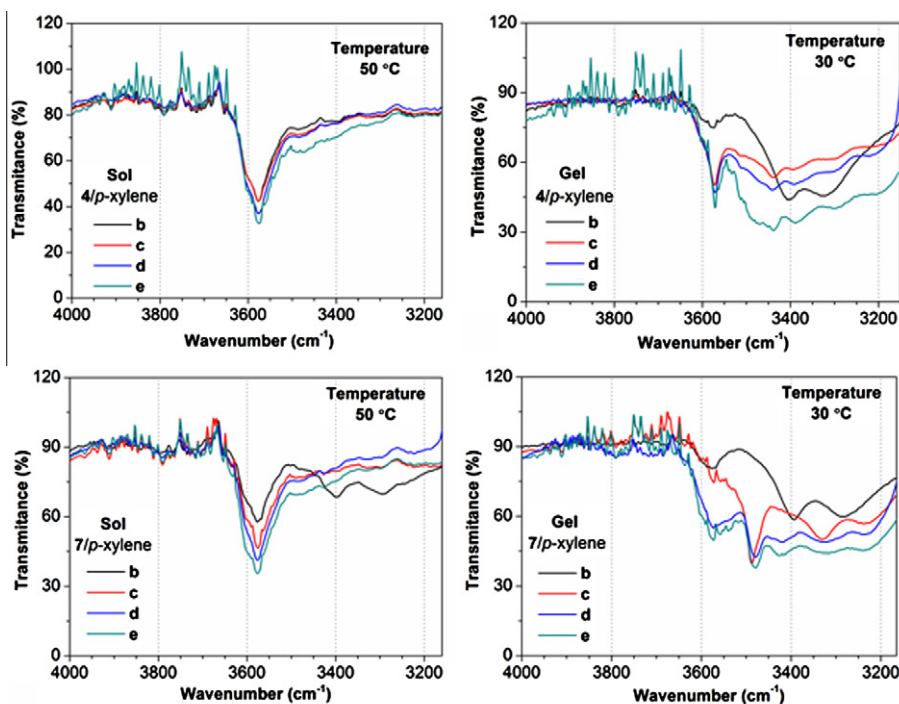


Figure 3. FTIR transmittance spectra of the gels **4b–e** (up) and **7b–e** (bottom) in *p*-xylene (30 mmol L⁻¹) at 50 °C (sol, at left) and 30 °C (gel, at right).

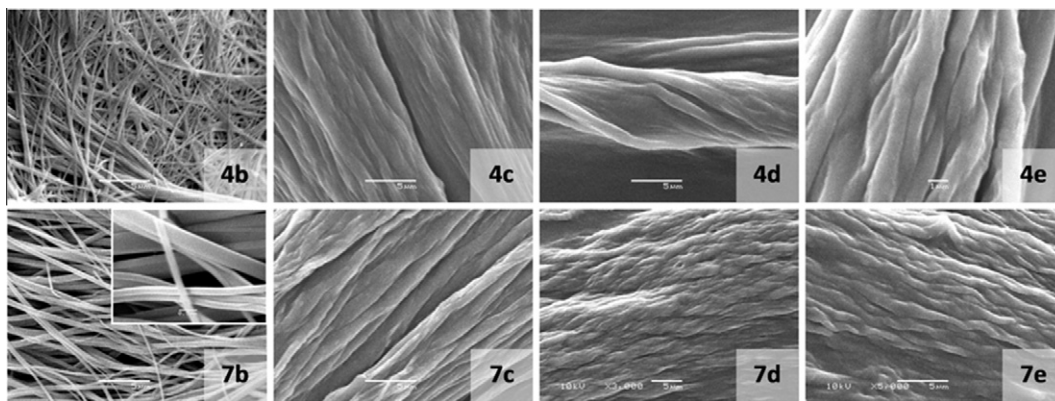


Figure 4. SEM images of the xerogel prepared from **4b–e** (up) and **7b–e** (bottom) in *p*-xylene.

of the solvent as can be observed from Figure 4. The morphology adopted is preferentially the cylindrical or tape-like organized aggregates. They have approximately 500 nm width for **4b** and **7b**, and 1 μm for **4c–e** and **7c–e**. They are also hundreds of micrometers in length, which is characteristic of one-dimensional stacking and anisotropic self-assembly. It is worth noting that fibers forming the tangled network are composed of various fibrils.²⁶ This type of secondary self-assembly among fibers justifies the large diameter of microfibers observed for the organogelators with long chain alkyl group, for example, **16 C** in **4e** and **7e**. No significant difference was observed among the two series, just the increasing in the fiber diameter with the growth of the alkyl chain.

2.5. DSC analyses

The thermal behavior of the organogels formed by **4b–e** and **7b–e** in *p*-xylene was investigated using differential scanning calorimetry (DSC)²⁷ and results are presented in Figure 5 as plots of T_{gel} versus gelator concentration. In general it was observed that sol–gel transition temperature increases with the molar concentration and decreases with alkyl chain size in both series of the gelators. Curiously, this last behavior is in accordance with the melting point found for the solid compounds. The gelators with shorter alkyl chain showed the higher melting points (mp **4b** 146 °C, **4c** 141 °C, **4d** 137 °C, **4e** 130 °C, and **7b** 148 °C, **7c** 146 °C, **7d** 138 °C, **7e** 132 °C). Finally, cycles of cooling/heating could be carried out without any loss in gelation ability or modification on T_{gel} , proving the process thermoreversibility and that any thermal history can be easily erased by heating above T_{gel} . The effect of thermal hysteresis presented in Figure 6 is common in gels and the obtained

results also confirm the thermoreversibility of the organogelators. Although large alkyl chain LMOG derivatives present a broader capability of solvent immobilization, as seen in gelation tests, small alkyl chain LMOG derivatives present higher T_{gel} . Both results, and also FTIR analyses, indicate that though van der Waals interaction plays an important role in gel formation, the hydrogen bonding is the driving force in self assembling and fibril structural maintenance. Alkyl chain lengthening obstructs or limits hydrogen bond interactions in the fibrils, reducing T_{gel} , but the raise of van der Waals interactions among distinct fibrils during the building of the secondary structure helps to immobilize a greater number of solvent molecules, even polar protic ones. In other words, the gelators with short alkyl chain undergo a more ordered molecular stacking during self-organization process than the gelators with long alkyl chains do. These results are in agreement with the microscopic observations (**7b**, Fig. 4, expanded view), where the short alkyl chain gelator built visually more compact network, that is, the adopted morphology of the fibers appears more regularly arranged.

2.6. SAXS analyses

Results obtained by SEM analyses supported the use Guinier's (Eq. 1), appropriate for cylindrical-shaped systems.²⁸

$$I = \frac{\{\varphi(\pi \cdot r \cdot \Delta\rho)^2\}}{q} \cdot \exp\left(\frac{-q^2 r^2}{4}\right) \quad (1)$$

where, φ is the concentration of gelator, r is radius of gyration, $\Delta\rho$ is the electronic density contrast between the aggregates and the surrounding medium. Thus, angular coefficient ($-r^2/4$) obtained in

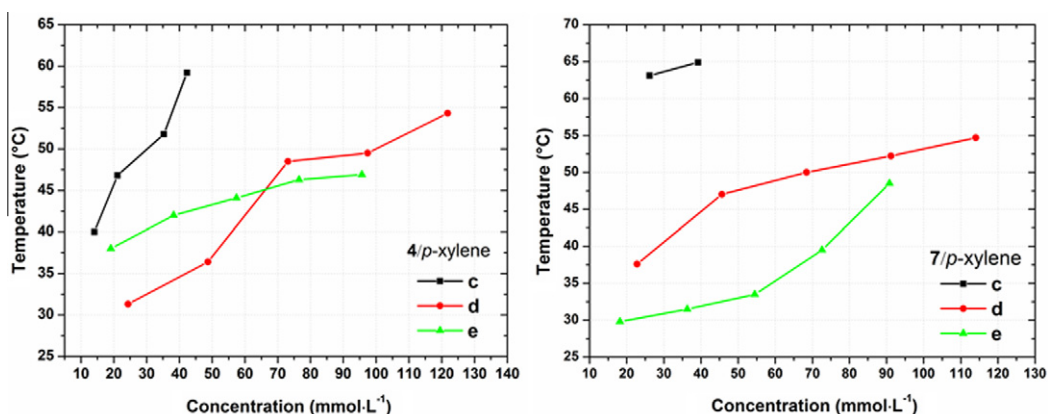


Figure 5. DSC curves of the T_{gel} for gels of **4c–e** (left) and **7c–e** in (right) *p*-xylene at different concentrations (mmol L^{-1}).

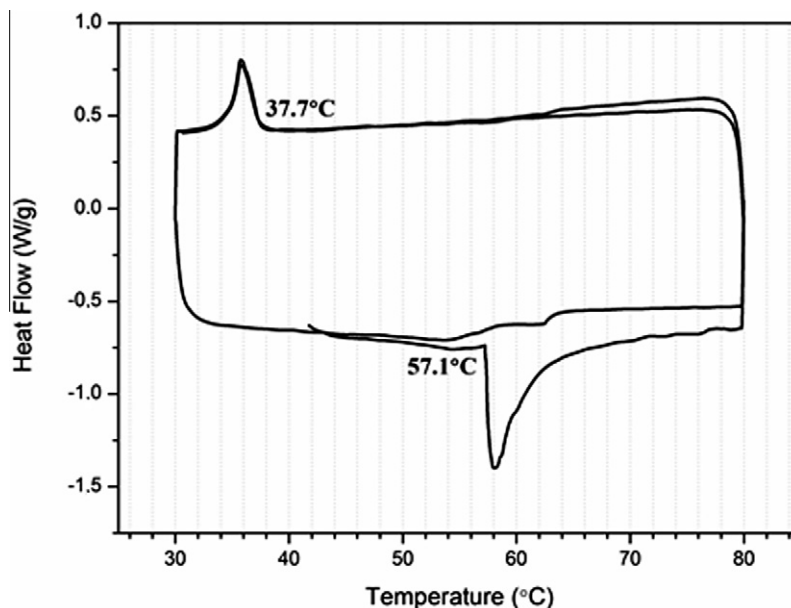


Figure 6. Heating and cooling cycles in a DSC thermogram of gel **4e** in *p*-xylene at 20 mmol L⁻¹.

the linear region by plotting a graph of $\ln(I/q)$ vs q^2 , gives the radius of the fiber for cylindrical aggregates.²⁹ Once the images obtained by SEM show the presence of cylindrical aggregates, the radius of gyration can be determined by using Guinier equation. As can be observed from Figures 7 and 8 for gels **4c–e** and **7c–e** in *p*-xylene, the profile showed a range of linear and angular coefficients in that region indicating the existence of a polydisperse system possessing nanofibers with different radii. These data are in

agreement with the SEM, which also showed different diameters for microfibers. When gelators of both series were compared, no significant change in relation to size of alkyl chain was observed, except the fiber of the gel **7e**/*p*-xylene that showed a slight increase in its radius, that is, 4.8–9.9 nm. Likewise, the increase in concentration did not result in any prominent change. Therefore, only the estimation of radius of the fiber in gel phase was possible under the adopted conditions.

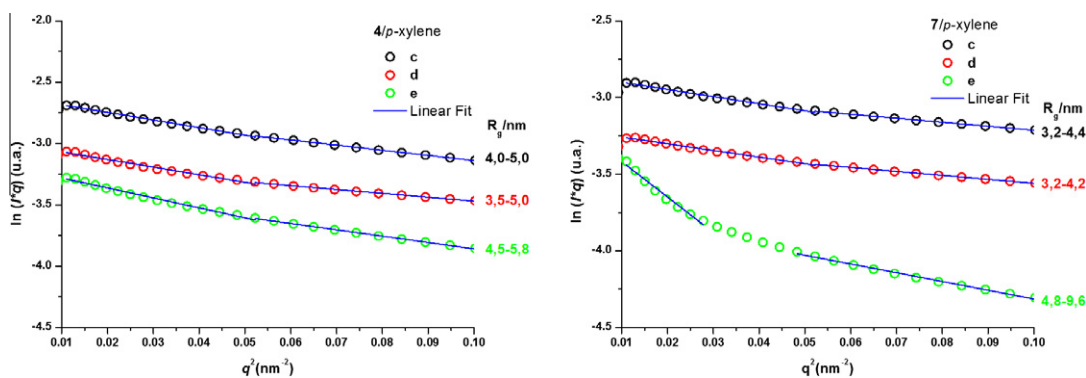


Figure 7. Photograph SAXS data plots for gels of **4c–e** and **7c–e**, in *p*-xylene at 30 mmol L⁻¹.

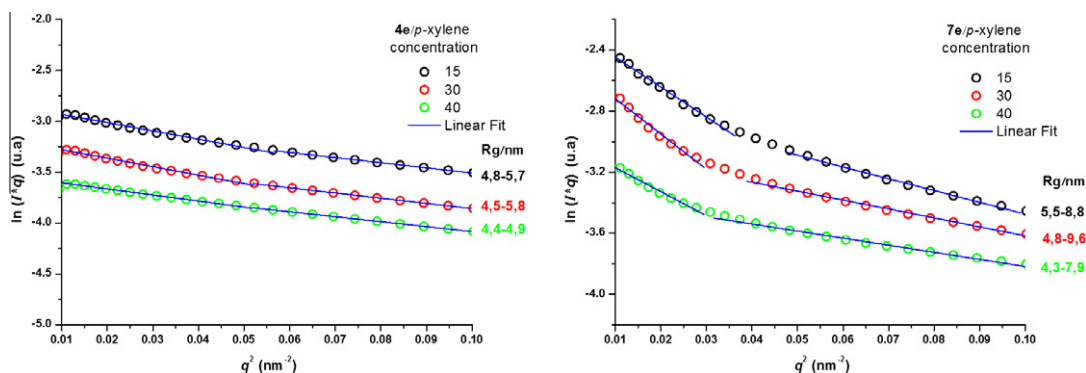


Figure 8. Photograph SAXS data plots for gels of **4e** and **7e** in *p*-xylene at 15, 30 and 40 mmol L⁻¹.

3. Conclusion

This study has demonstrated that among several methyl 4, 6-*O*-benzylidene α -D-glucopyranosides (**4b–e** and **7b–e**) acting as efficient gelators for diverse organic solvents, the hydrogen-bond remains to be the main driving force for self-assembly despite alkyl chain size lengthening or electron density at the aromatic ring. Nevertheless, van der Waals interaction plays an important role in broadening the scope of solvent immobilization as long chain derivatives were capable of gelling even polar protic ones. Calorimetry showed T_{gel} increases with the molar concentration but decreases with alkyl chain size in both series of the gelators, which was interpreted as being a hurdled self assemblage with alkyl chain lengthening. DSC analyses also showed well defined peaks during sol–gel transition that is coherent with hydrogen bond driven assembling. FTIR spectroscopy positively confirmed that the chief intermolecular interaction among gelator molecules in both series (**4b–e** and **7b–e**) during gel formation is the hydrogen bond, despite the implemented structural modifications. SAXS study showed a polydisperse system possessing nanofibers with different radii. There was no significant change in radii among gelators of both series, although LMOG with larger alkyl chains presented larger radii suggesting a higher tendency for fibril merging in larger alkyl chain derivatives. As described elsewhere, a one-dimensional intermolecular hydrogen bonding network to both hydroxyl groups must occur for efficient formation of a gel.^{14a} In addition of such requirement the presence of junction nodes and the enhancement of fiber thickness are also important to improve the organogelator efficiency. The occurrence of these characteristics permits D-mannose or D-galactose 4,6-*O*-benzylidene derivatives to be better gelators than D-glucose derivatives.^{14a} Nevertheless, the attachment of large alkyl groups promoted merging among different fibrils creating a van der Waals based three-dimensional fiber network with hydrogen bonded based fibers, helping to immobilize a greater number of solvents. Despite this secondary interaction, the supramolecular core stands fibrillar and undergoes self-assemblage by hydrogen bonds, following the model described elsewhere.^{14a–d} We believe that the abovementioned findings may be useful for discovery, design, or improvement of new gelators. This opens up the possibility that the carbohydrate library provided by nature can be modified even further, in particular to the rational design of molecular assemblies with a very defined function.

4. Experimental section

4.1. Synthesis of compounds

4.1.1. Methyl α -D-glucopyranoside (**1**)

Prepared as described elsewhere and isolated as white solid: mp 165–166 °C (lit. 164–165 °C).¹⁸ IR (KBr, cm^{-1}): ν 3600–3050, 3547, 2915, 1036; ^1H NMR (400 MHz, D_2O) δ (ppm): 4.73 (d, 1H, $J_{1-2} = 3.6$ Hz, H-1), 3.77–3.81 (m, 1H), 3.65–3.69 (m, 1H), 3.54–3.60 (m, 2H), 3.46–3.49 (m, 1H), 3.33 (s, 3H, OCH₃), 3.29–3.31 (m, 1H); ^{13}C NMR (100 MHz, D_2O) δ (ppm) 99.3, 73.1, 71.6, 71.2, 69.5, 60.5, 55.0. TOF-MS, m/z calculated for $\text{C}_6\text{H}_{11}\text{O}_5^+[\text{M}-\text{OCH}_3]^+$ 163.0607, found: m/z 163.0636.

4.1.1.1. Compounds 2a–e.¹⁹ 4-Hydroxybenzaldehyde (244 mg, 2 mmol) was added to a solution of 46 mg (2 mmol) of sodium ethoxide in 12 mL of ethanol and stirred until completely consumed. Solution was kept under reflux (70 °C) with magnetic stirring for 20 min. The corresponding alkylation agent (*n*-alkyl bromide, 2 mmol) was added to the system and the temperature was maintained at 70 °C with stirring for 48 h. Compounds **2a–d** were isolated by solvent extraction (ethyl acetate/water, 3:1) and then purified by

distillation. Compound **2e** was fussyly purified by flash chromatography in silica gel (hexane/ethyl acetate; 95:05, R_f 0.4).

Compound **2a** (73% yield); IR (NaCl, cm^{-1}): ν 2985, 2935, 2738, 1692, 1260, 1163, 1040, 836; ^1H NMR (250 MHz, CDCl_3 , TMS) δ (ppm): 9.87 (s, 1H), 7.82 (d, 2H, $J = 8.9$ Hz), 6.98 (d, 2H, $J = 8.6$ Hz), 4.12 (q, 2H, $J = 7.0$ Hz), 1.45 (t, 3H, $J = 7.0$ Hz); EI-MS, m/z 150 $[\text{M}]^+$, 121 $[\text{HO}-\text{C}_6\text{H}_4-\text{C}\equiv\text{O}]^+$, 93 $[\text{HO}-\text{C}_6\text{H}_4]^+$. Compound **2b** (75% yield); IR (NaCl, cm^{-1}): ν 2967, 2876, 2734, 1692, 1602, 1261, 1160, 834; ^1H NMR (250 MHz, CDCl_3 , TMS) δ (ppm): 9.88 (s, 1H), 7.82 (d, 2H, $J = 8.8$ Hz), 6.99 (d, 2H, $J = 8.8$ Hz), 4.00 (t, 2H, $J = 6.5$ Hz), 1.85 (h, 2H, $J = 7.3$ Hz), 1.05 (t, 3H, $J = 7.5$ Hz); EI-MS, m/z 164 $[\text{M}]^+$, 121 $[\text{HO}-\text{C}_6\text{H}_4-\text{C}\equiv\text{O}]^+$, 93 $[\text{HO}-\text{C}_6\text{H}_4]^+$. Compound **2c** (73% yield); IR (NaCl, cm^{-1}): ν 2964, 2872, 2733, 1692, 1600, 1260, 1158, 828; ^1H NMR (250 MHz, CDCl_3 , TMS) δ (ppm): 9.87 (s, 1H), 7.82 (d, 2H, $J = 8.8$ Hz), 6.99 (d, 2H, $J = 8.7$ Hz), 4.04 (t, 2H, $J = 6.5$ Hz), 1.80 (p, 2H, $J = 6.9$ Hz), 1.50 (h, 2H, $J = 7.5$ Hz), 0.99 (t, 3H, $J = 7.3$ Hz); EI-HRMS, calculated for $\text{C}_{11}\text{H}_{14}\text{O}_2$ m/z 178.0994, found: m/z 178.0898 $[\text{M}]^+$, 121.0211 $[\text{HO}-\text{C}_6\text{H}_4-\text{C}\equiv\text{O}]^+$ (calcd 121.0290), 93.0286 $[\text{HO}-\text{C}_6\text{H}_4]^+$ (calcd 93.0340). Compound **2d** (66% yield); IR (NaCl, cm^{-1}): ν 2931, 2856, 2741, 1697, 1600, 1254, 1156, 832; ^1H NMR (250 MHz, CDCl_3 , TMS) δ (ppm): 9.87 (s, 1H), 7.83 (d, 2H, $J = 8.8$ Hz), 6.99 (d, 2H, $J = 8.7$ Hz), 4.03 (t, 2H, $J = 6.5$ Hz), 1.81 (p, 2H), 1.29–1.52 (m, 10H), 0.89 (t, 3H, $J = 6.6$ Hz); EI-MS, m/z 234 $[\text{M}]^+$, 121 $[\text{HO}-\text{C}_6\text{H}_4-\text{C}\equiv\text{O}]^+$, 93 $[\text{HO}-\text{C}_6\text{H}_4]^+$. Compound **2e** (isolated as a white solid, mp 44 °C, in 73% yield); IR (KBr, cm^{-1}): ν 2913, 2852, 2730, 1691, 1603, 1255, 1174, 837; ^1H NMR (250 MHz, CDCl_3 , TMS) δ (ppm): 9.88 (s, 1H), 7.82 (d, 2H, $J = 8.8$ Hz), 6.99 (d, 2H, $J = 8.8$ Hz), 4.03 (t, 2H, $J = 6.5$ Hz), 1.81 (p, 2H, $J = 6.7$ Hz), 1.26–1.49 (m, 26H), 0.88 (t, 3H, $J = 6.9$ Hz); EI-HRMS, calculated for $\text{C}_{23}\text{H}_{38}\text{O}_2$ m/z 346.2872, found: m/z 346.2749 $[\text{M}]^+$, 121.0077 $[\text{HO}-\text{C}_6\text{H}_4-\text{C}\equiv\text{O}]^+$ (calcd 121.0290).

4.1.1.2. Compounds 5a–e.²⁰ To a mixture of 4-formylbenzoic acid (1.5 g, 0.01 mol) and potassium carbonate (2.76 g, 0.02 mol) in dry *N,N*-dimethylformamide (30 mL), the corresponding *n*-alkyl bromide was added. The solution was maintained at 70 °C under magnetic stirring for 12 h. The solvent was evaporated under reduced pressure and the product was separated by solvent extraction (dichloromethane/water, 50:10 mL). The organic phase was dried with anhydrous sodium sulfate and evaporated under reduced pressure furnishing yellowish liquids for compounds **5a–d** and a white solid for **5e**. Compounds **5a–d** were purified by distillation leading to the formation of colorless products and compound **5e** was purified flash chromatography in silica gel (hexane/ethyl acetate; 95:05, R_f 0.3).

Compound **5a** (73% yield); IR (NaCl, cm^{-1}): ν 2975, 2837, 2732, 1721, 1709, 1275, 1102, 764; ^1H NMR (250 MHz, CDCl_3 , TMS) δ (ppm): 10.10 (s, 1H), 8.20 (d, 2H, $J = 8.2$ Hz), 7.95 (d, 2H, $J = 8.5$ Hz), 4.42 (q, 2H, $J = 7.0$ Hz), 1.42 (t, 2H, $J = 7.2$ Hz); EI-MS, m/z 178 $[\text{M}]^+$, 149 $[\text{HO}_2\text{C}-\text{C}_6\text{H}_4-\text{C}\equiv\text{O}]^+$, 133 $[\text{O}=\text{C}-\text{C}_6\text{H}_4-\text{CHO}]^+$. Compound **5b** (75% yield); IR (NaCl, cm^{-1}): ν 2976, 2879, 2734, 1721, 1708, 1272, 1104, 762; ^1H NMR (250 MHz, CDCl_3 , TMS) δ (ppm): 10.07 (s, 1H), 8.20 (d, 2H, $J = 8.5$ Hz), 7.95 (d, 2H, $J = 8.2$ Hz), 4.32 (t, 2H, $J = 6.7$ Hz), 1.82 (h, 2H, $J = 7.2$ Hz), 1.04 (t, 3H, $J = 7.5$ Hz); EI-MS, m/z 192 $[\text{M}]^+$, 151 $[\text{H}_2\text{O}_2\text{C}-\text{C}_6\text{H}_4-\text{CHO}]^+$, 133 $[\text{O}=\text{C}-\text{C}_6\text{H}_4-\text{CHO}]^+$. Compound **5c** (82% yield); IR (NaCl, cm^{-1}): ν 2957, 2879, 2734, 1722, 1709, 1282, 1106, 759; ^1H NMR (250 MHz, CDCl_3 , TMS) δ (ppm): 10.10 (s, 1H), 8.20 (d, 2H, $J = 8.3$ Hz), 7.95 (d, 2H, $J = 8.4$ Hz), 4.36 (t, 2H, $J = 6.7$ Hz), 1.78 (p, 2H, $J = 7.2$ Hz), 1.50 (h, 2H, $J = 7.3$ Hz), 0.98 (t, 3H, $J = 7.3$ Hz); EI-MS, m/z 205 $[\text{M}-\text{H}]^+$, 151 $[\text{H}_2\text{O}_2\text{C}-\text{C}_6\text{H}_4-\text{CHO}]^+$, 133 $[\text{O}=\text{C}-\text{C}_6\text{H}_4-\text{CHO}]^+$. Compound **5d** (80% yield); IR (NaCl, cm^{-1}): ν 2963, 2852, 1721, 1279, 1110, 726; ^1H NMR (250 MHz, CDCl_3 , TMS) δ (ppm): 10.10 (s, 1H), 8.20 (d, 2H, $J = 8.3$ Hz), 7.95 (d, 2H, $J = 8.5$ Hz), 4.36 (t, 2H, $J = 6.7$ Hz), 1.79 (p, 2H, $J = 6.7$ Hz),

1.29–1.48 (m, 12H), 0.88 (t, 3H, $J = 6.5$ Hz); EI-MS, m/z 262[M]⁺, 151 [H₂O₂C–C₆H₄–CHO]⁺, 133 [O=C–C₆H₄–CHO]⁺. Compound **5e** (isolated as a white solid, mp 52 °C, in 61% yield); IR (KBr, cm^{−1}): ν 2960, 2916, 2854, 1724, 1282, 1124, 753; ¹H NMR (250 MHz, CDCl₃, TMS) δ (ppm): 10.10 (s, 1H), 8.20 (d, 2H, $J = 8.3$ Hz), 7.95 (d, 2H, $J = 8.4$ Hz), 4.35 (t, 2H, $J = 6.7$ Hz), 1.78 (p, 2H, $J = 6.9$ Hz), 1.25–1.47 (m, 26H), 0.88 (t, 3H, $J = 6.3$ Hz); EI-HRMS, calculated for C₂₄H₃₈O₃ m/z 374.2821, found: m/z 374.2845 [M]⁺, 151.0409 [H₂O₂C–C₆H₄–CHO]⁺ (calcd 151.0395), 133.0285 [O=C–C₆H₄–CHO]⁺ (calcd 133.0290).

4.1.1.3. Compounds 3a–e and 6a–e²¹ Starting material (0.01 mol of **2a–e** or **5a–e**) and trimethyl orthoformate (1.59 g, 0.015 mol) in 1.5 mL of methanol were stirred at room temperature. Two drops of concentrated hydrochloric acid were added to this solution. Procedures for compounds **2a–d** were left under stirring for two days at room temperature, and reactions with compounds **5a–d** were kept for only 6 h under agitation at room temperature. Nevertheless, compounds **2e** and **5e** were prepared similarly to their analogues, but under somewhat higher temperature (50 °C) and longer reaction times (four days). After these periods, all products were isolated by neutralization with KOH dissolved in methanol followed by evaporation of volatiles under reduced pressure, and extraction with ethyl ether and water (8 mL, 3:1). Organic phases were dried over anhydrous Na₂SO₄ followed by volatile removing on rotary evaporator. The compounds **3a–d** and **6a–d** were purified by distillation at reduced pressure resulting in colorless liquids. Compounds **3e** and **6e** were purified by flash chromatography in silica gel (hexane/ethyl acetate, 95:05, R_f 0.5 and 0.4, respectively).

Compound **3a** (81% yield); IR (NaCl, cm^{−1}): ν 2983, 2821, 1610, 1512, 1242, 1052, 830; ¹H NMR (250 MHz, CDCl₃, TMS) δ (ppm): 7.35 (d, 2H, $J = 8.5$ Hz), 6.88 (d, 2H, $J = 8.8$ Hz), 5.34 (s, 1H), 4.03 (q, 2H, $J = 7.0$ Hz), 3.30 (s, 6H), 1.41 (t, 3H, $J = 7.0$ Hz); EI-MS, m/z 196 [M]⁺, 165 [CH₃O=CH–C₆H₄–OC₂H₅]⁺, 150 [O=CH–C₆H₄–OC₂H₅]⁺. Compound **3b** (70% yield); IR (NaCl, cm^{−1}): ν 2964, 2825, 1611, 1513, 1246, 1055, 831; ¹H NMR (250 MHz, CDCl₃, TMS) δ (ppm): 7.36 (d, 2H, $J = 8.6$ Hz), 6.88 (d, 2H, $J = 8.7$ Hz), 5.34 (s, 1H), 3.92 (t, 2H, $J = 6.5$ Hz), 3.30 (s, 6H), 1.80 (h, 2H, $J = 7.3$ Hz), 1.03 (t, 3H, $J = 7.4$ Hz); EI-MS, m/z 210.1[M]⁺, 179.1 [CH₃O=CH–C₆H₄–OC₃H₇]⁺, 164.1 [O=CH–C₆H₄–OC₃H₇]⁺. Compound **3c** (62% yield); IR (NaCl, cm^{−1}): ν 2957, 2820, 1610, 1507, 1242, 1055, 818; ¹H NMR (250 MHz, CDCl₃, TMS) δ (ppm): 7.34 (d, 2H, $J = 8.7$ Hz), 6.88 (d, 2H, $J = 8.8$ Hz), 5.34 (s, 1H), 3.96 (t, 2H, $J = 6.5$ Hz), 3.31 (s, 6H), 1.76 (p, 2H, $J = 6.6$ Hz), 1.49 (h, 2H, $J = 7.5$ Hz), 0.97 (t, 3H, $J = 7.3$ Hz); EI-HRMS, m/z calculated for C₁₂H₁₇O₂ [M–OCH₃]⁺ = [CH₃O=CH–C₆H₄–OC₄H₉]⁺ m/z 193.1229, found: m/z 193.1203, 178.0967 [O=CH–C₆H₄–OC₄H₉]⁺ (calcd 178.0994). Compound **3d** (73% yield); IR (NaCl, cm^{−1}): ν 2928, 2828, 1617, 1512, 1242, 1057, 826; ¹H NMR (250 MHz, CDCl₃, TMS) δ (ppm): 7.35 (d, 2H, $J = 8.6$ Hz), 6.88 (d, 2H, $J = 8.6$ Hz), 5.34 (s, 1H), 3.94 (t, 2H, $J = 6.5$ Hz), 3.31 (s, 6H), 1.77 (p, 2H, $J = 6.6$ Hz), 1.28–1.47 (m, 10H), 0.88 (t, 3H, $J = 6.3$ Hz); EI-HRMS, calculated for C₁₇H₂₈O₃ m/z 280.2038, found: m/z 280.2093 [M]⁺, 249.1814 [CH₃O=CH–C₆H₄–OC₈H₁₇]⁺ (calcd 249.1855), 234.1648 [O=CH–C₆H₄–OC₈H₁₇]⁺ (calcd 234.1620). Compound **3e** (isolated as a white solid, mp 42 °C, in 71% yield); IR (KBr, cm^{−1}): ν 2916, 2846, 1620, 1517, 1246, 1049, 808; ¹H NMR (250 MHz, CDCl₃, TMS) δ (ppm): 7.34 (d, 2H, $J = 8.6$ Hz), 6.87 (d, 2H, $J = 8.7$ Hz), 5.41 (s, 1H), 3.97 (t, 2H, $J = 6.6$ Hz), 3.31 (s, 6H), 1.77 (p, 2H, $J = 6.5$ Hz), 1.26–1.47 (m, 26H), 0.88 (t, 3H, $J = 6.2$ Hz); EI-MS, m/z 361.3 [CH₃O=CH–C₆H₄–OC₁₆H₃₃]⁺, 346.3 [O=CH–C₆H₄–OC₁₆H₃₃]⁺.

Compound **6a** (86% yield); IR (NaCl, cm^{−1}): ν 2982, 2827, 1714, 1277, 1105, 1062, 761; ¹H NMR (250 MHz, CDCl₃, TMS) δ (ppm): 8.00 (d, 2H, $J = 8.4$ Hz), 7.50 (d, 2H, $J = 8.0$ Hz), 5.44 (s, 1H), 4.38 (q, 2H, $J = 7.2$ Hz), 3.33 (s, 6H), 1.40 (t, 3H, $J = 7.1$ Hz); EI-MS, m/z 223 [M–H]⁺, 193 [CH₃O=CH–C₆H₄–CO₂C₂H₅]⁺, 179 [H(CH₃O)₂C–

C₆H₄–C=O]⁺. Compound **6b** (85% yield); IR (NaCl, cm^{−1}): ν 2974, 2828, 1719, 1279, 1106, 1056, 762; ¹H NMR (250 MHz, CDCl₃, TMS) δ (ppm): 8.05 (d, 2H, $J = 8.3$ Hz), 7.50 (d, 2H, $J = 8.3$ Hz), 5.44 (s, 1H), 4.28 (t, 2H, $J = 6.7$ Hz), 3.33 (s, 6H), 1.80 (h, 2H, $J = 7.2$ Hz), 1.03 (t, 3H, $J = 7.4$ Hz); EI-MS, m/z 207 [CH₃O=CH–C₆H₄–CO₂C₃H₇]⁺, 179 [H(CH₃O)₂C–C₆H₄–C=O]⁺. Compound **6c** (77% yield); IR (NaCl, cm^{−1}): ν 2990, 2832, 1724, 1280, 1105, 1056, 761; ¹H NMR (250 MHz, CDCl₃, TMS) δ (ppm): 8.04 (d, 2H, $J = 8.4$ Hz), 7.52 (d, 2H, $J = 8.1$ Hz), 5.44 (s, 1H), 4.32 (t, 2H, $J = 6.5$ Hz), 3.33 (s, 6H), 1.76 (p, 2H, $J = 7.0$ Hz), 1.48 (h, 2H, $J = 7.8$ Hz), 0.98 (t, 3H, $J = 7.3$ Hz); EI-MS, m/z 251 [M–H]⁺, 221 [CH₃O=CH–C₆H₄–CO₂C₄H₉]⁺, 179 [H(CH₃O)₂C–C₆H₄–C=O]⁺. Compound **6d** (75% yield); IR (NaCl, cm^{−1}): ν 2956, 2860, 1722, 1267, 1106, 1060, 759; ¹H NMR (250 MHz, CDCl₃, TMS) δ (ppm): 8.05 (d, 2H, $J = 8.4$ Hz), 7.53 (d, 2H, $J = 8.3$ Hz), 5.44 (s, 1H), 4.31 (t, 2H, $J = 6.7$ Hz), 3.33 (s, 6H), 1.77 (p, 2H, $J = 7.2$ Hz), 1.28–1.46 (m, 10H), 0.88 (t, 3H, $J = 7.0$ Hz); EI-MS, m/z 277.1 [CH₃O=CH–C₆H₄–CO₂C₈H₁₇]⁺, 179 [H(CH₃O)₂C–C₆H₄–C=O]⁺. Compound **6e** (isolated as a white solid, mp 48 °C, in 73% yield); IR (KBr, cm^{−1}): ν 2955, 2854, 1719, 1273, 1105, 1050, 759; ¹H NMR (250 MHz, CDCl₃, TMS) δ (ppm): 8.04 (d, 2H, $J = 8.3$ Hz), 7.53 (d, 2H, $J = 8.1$ Hz), 5.44 (s, 1H), 4.31 (t, 2H, $J = 6.6$ Hz), 3.33 (s, 6H), 1.76 (p, 2H, $J = 7.0$ Hz), 1.23 (m, 26H), 0.88 (t, 3H, $J = 6.7$ Hz); EI-HRMS, m/z calculated for C₂₅H₄₁O₃ [M–OCH₃]⁺ 389.3056, found: m/z 389.3113 [CH₃O=CH–C₆H₄–CO₂C₁₆H₃₃]⁺, 374.3141 [O=CH–C₆H₄–CO₂C₁₆H₃₃]⁺ (calcd 374.2821).

4.1.1.4. Compounds 4a–e and 7a–e²² Methyl α -D-glucopyranoside (**1**, 0.97 g, 5 mmol), dimethylacetal derivatives **3a–e** or **6a–e** (5 mmol), dry *N,N*-dimethylformamide (4 mL), and *p*-toluenesulfonic acid monohydrate (*p*-TSA, 2.5 mg) were mixed and heated at 80 °C for 4–6 h. Then, DMF was evaporated under reduced pressure, and a solution of 2% NH₄OH (5 mL) was added to the residue. The resulting suspension was stirred and heated at 80 °C for 1 h, and after that cooled in an ice bath. The final product was filtered off and washed with distilled water (3 × 10 mL), resulting in a white solid which was dried in a high vacuum pump at room temperature. Compounds **4a** and **7a** were purified by recrystallization from ethyl acetate, and the other ones were purified by column chromatography in silica gel with dichloromethane/ethyl acetate 3:1 (**4b** and **7b**), or alumina with dichloromethane/methanol 95:05 (**4c–e** and **7c–e**).

Compound **4a** (isolated as white needle-like crystals in 66% yield, mp 188–190 °C, $[\alpha]_D^{20}$

+85 (c 0.5 g/100 mL, MeOH); IR (KBr, cm^{−1}): ν 3180–3616, 2997, 2848, 1617, 1513, 1376, 1255, 1076, 1039, 820; ¹H NMR (250 MHz, DMSO-*d*₆, TMS) δ (ppm): 7.34 (d, 2H, $J_{9-10} = 8.7$ Hz, H-9), 6.89 (d, 2H, $J_{10-9} = 8.7$ Hz, H-10), 5.49 (s, 1H, H-7), 5.16 (d, 1H, $J_{OH-3} = 5.0$ Hz, OH), 4.98 (d, 1H, $J_{OH-2} = 6.5$ Hz, OH), 4.63 (d, 1H, $J_{1-2} = 3.7$ Hz, H-1), 4.13 (dd, 1H, $J_{6B-5} = 4.1$ Hz, $J_{6B-6A} = 9.5$ Hz, H-6B), 4.01 (q, 2H, $J_{12-13} = 7.5$ Hz, H-12), 3.62–3.70 (m, 1H, H-6A), 5.52–3.62 (m, 2H, H-3, H-5), 3.34–3.37 (m, 2H, H-2, H-4), 3.33 (s, 3H, OCH₃), 1.31 (t, 3H, H-13); ¹³C NMR (62.5 MHz, DMSO-*d*₆, TMS) δ (ppm): 158.7, 129.9, 127.6, 113.6, 100.7, 100.4, 81.2, 72.3, 69.8, 68.0, 62.9, 62.3, 54.6, 14.5; TOF-MS, m/z calculated for C₁₆H₂₂O₇ 326.1366, found: m/z 326.1366. Compound **4b** (isolated as a white solid in 75% yield, mp 146–148 °C, $[\alpha]_D^{20}$ +83 (c 0.6 g/100 mL, MeOH); IR (KBr, cm^{−1}): ν 3196–3608, 2987, 2864, 1619, 1516, 1373, 1247, 1071, 1037, 802; ¹H NMR (400 MHz, DMSO-*d*₆, TMS) δ (ppm): 7.34 (d, 2H, $J_{9-10} = 8.8$ Hz, H-9), 6.90 (d, 2H, $J_{10-9} = 8.8$ Hz, H-10), 5.49 (s, 1H, H-7), 5.16 (d, 1H, $J_{OH-3} = 5.2$ Hz, OH), 4.98 (d, 1H, $J_{OH-2} = 6.8$ Hz, OH), 4.62 (d, 1H, $J_{1-2} = 3.6$ Hz, H-1), 4.13 (dd, 1H, $J_{6B-5} = 4.4$ Hz, $J_{6B-6A} = 9.8$ Hz, H-6B), 3.91 (t, 2H, $J_{12-13} = 6.8$ Hz, H-12), 3.66 (t, 1H, $J_{6A-6B, 6A-5} = 10.0$ Hz), 3.53–3.59 (m, 2H, H-3, H-5), 3.31–3.36 (m, 2H, H-2, H-4), 3.33 (s, 3H, OCH₃), 1.73 (h, 2H, $J_{13} = 7.2$ Hz, H-13), 0.96 (t, 3H, $J_{14} = 7.4$ Hz, 8.3 Hz, H-14);

^{13}C NMR (100 MHz, DMSO- d_6 , TMS) δ (ppm): 158.9, 130.1, 127.7, 113.8, 100.8, 100.5, 81.3, 72.4, 69.9, 68.9, 68.1, 62.4, 54.7, 22.0, 10.3; TOF-MS, m/z calculated for $\text{C}_{17}\text{H}_{24}\text{O}_7$ 340.1522, found: m/z 340.1518. Compound **4c** (isolated as a white solid in 69% yield, mp 141–142 °C, $[\alpha]_D^{20} +84$ (c 0.6 g/100 mL, MeOH); IR (KBr, cm^{-1}): ν = 3134–3606, 2962, 2869, 1616, 1516, 1373, 1245, 1079, 1030, 827; ^1H NMR (400 MHz, CDCl_3 , TMS) δ (ppm): 7.41 (d, 2H, J_{9-10} = 8.8 Hz, H-9), 6.89 (d, 2H, J_{10-9} = 8.8 Hz, H-10), 5.49 (s, 1H, H-7), 4.78 (d, 1H, J_{1-2} = 3.9 Hz, H-1), 4.28 (dd, 1H, J_{6B-5} = 4.3 Hz, J_{6B-6A} = 9.7 Hz, H-6B), 3.96 (t, 2H, J_{12-13} = 6.5 Hz, H-12), 3.89–3.94 (m, 1H, H-3), 3.70–3.83 (m, 2H, H-5, H-6A), 3.58–3.64 (m, 1H, H-2), 3.45–3.49 (m, 1H, H-4), 3.46 (s, 3H, OCH_3), 3.05 (s, 1H, OH), 2.53 (d, 1H, $J_{\text{OH}-2}$ = 9.2 Hz, OH), 1.77 (p, 2H, J_{13-14} = 6.6 Hz, H-13), 1.49 (h, 2H, J_{14-15} = 7.5 Hz, H-15), 0.98 (t, 3H, J_{15-14} = 7.4 Hz, H-15); ^{13}C NMR (100 MHz, CDCl_3 , TMS) δ (ppm): 159.8, 129.3, 127.6, 114.3, 101.9, 99.8, 80.9, 72.8, 71.7, 68.9, 67.7, 62.4, 55.5, 31.2, 19.2, 13.8; TOF-MS, m/z calculated for $\text{C}_{18}\text{H}_{26}\text{O}_7$ 354.1578, found: m/z 354.1663. Compound **4d** (isolated as a white solid in 66% yield, mp 137–138 °C, $[\alpha]_D^{20} +63$ (c 0.6 g/100 mL, MeOH); IR (KBr, cm^{-1}): ν = 3154–3615, 2926, 2852, 1622, 1513, 1380, 1251, 1079, 1031, 823; ^1H NMR (400 MHz, CDCl_3 , TMS) δ (ppm): 7.39 (d, 2H, J_{9-10} = 8.7 Hz, H-9), 6.86 (d, 2H, J_{10-9} = 8.7 Hz, H-10), 5.46 (s, 1H, H-7), 4.75 (d, 1H, J_{1-2} = 3.9 Hz, H-1), 4.25 (dd, 1H, J_{6B-5} = 4.3 Hz, J_{6B-6A} = 9.7 Hz, H-6B), 3.93 (t, 2H, J_{12-13} = 6.6 Hz, H-12), 3.86–3.89 (m, 1H, H-3), 3.67–3.80 (m, 2H, H-5, H-6A), 3.56–3.61 (m, 1H, H-2), 3.41–3.46 (m, 1H, H-4), 3.43 (s, 3H, OCH_3), 3.15 (s, 1H, OH), 2.60 (d, 1H, $J_{\text{OH}-2}$ = 9.6 Hz, OH), 1.75 (p, 2H, J_{13-14} = 7.3 Hz, H-13), 1.28–1.47 (m, 10H, H-14–18), 0.88 (t, 3H, J_{19-18} = 7.4 Hz, H-19); ^{13}C NMR (62.5 MHz, CDCl_3 , TMS) δ (ppm): 160.0, 129.5, 127.7, 114.4, 102.1, 99.9, 81.1, 73.0, 71.8, 69.0, 68.2, 62.5, 55.6, 31.9, 29.5, 29.3, 26.1, 22.7, 14.2; TOF-MS, m/z calculated for $\text{C}_{22}\text{H}_{34}\text{O}_7$ 410.2305, found: m/z 410.2305. Compound **4e** (isolated as a white solid in 75% yield, mp 130–132 °C, $[\alpha]_D^{20} +56$ (c 0.6 g/100 mL, MeOH); IR (KBr, cm^{-1}): ν = 3145–3605, 2925, 2851, 1620, 1523, 1379, 1252, 1083, 1037, 827; ^1H NMR (400 MHz, DMSO- d_6 , TMS) δ (ppm): 7.33 (d, 2H, J_{9-10} = 8.6 Hz, H-9), 6.88 (d, 2H, J_{10-9} = 8.6 Hz, H-10), 5.48 (s, 1H, H-7), 4.90 (d, 1H, J_{1-2} = 4.9 Hz, H-1), 4.71 (d, 1H, $J_{\text{OH}-3}$ = 6.6 Hz, OH), 4.62 (d, 1H, $J_{\text{OH}-2}$ = 3.6 Hz, OH), 4.12 (dd, 1H, J_{6B-5} = 4.4 Hz, J_{6B-6A} = 9.8 Hz, H-6B), 3.95 (t, 2H, J_{12-13} = 6.5 Hz, H-12), 3.59–3.68 (m, 1H, H-6A), 3.54–3.61 (m, 2H, H-3, H-5), 3.32–3.40 (m, 1H, H-4), 3.33 (s, 3H, OCH_3), 3.15 (H_2O), 1.68 (p, 2H, J_{13-14} = 6.7 Hz, H-13), 0.85 (t, 3H, J_{27-26} = 6.2 Hz, H-27); ^{13}C NMR (62.5 MHz, DMSO- d_6 , TMS) δ (ppm): 158.9, 130.0, 127.6, 113.7, 100.8, 100.5, 81.3, 72.4, 69.9, 68.1, 67.4, 62.3, 54.7, 31.2, 28.9, 28.7, 28.6, 25.4, 22.0, 13.8; TOF-MS, m/z calculated for $\text{C}_{30}\text{H}_{50}\text{O}_7$ 522.3557, found: m/z 522.3553.

Compound **7a** (isolated as white needle-like crystals in 60% yield, mp 190–192 °C, $[\alpha]_D^{20} +61$ (c 0.48 g/100 mL, MeOH); IR (KBr, cm^{-1}): ν = 3137–3633, 2997, 2868, 1716, 1375, 1279, 1069, 1034, 762; ^1H NMR (400 MHz, DMSO- d_6 , TMS) δ (ppm): 7.97 (d, 2H, J_{9-10} = 8.5 Hz, H-9), 7.59 (d, 2H, J_{10-9} = 8.3 Hz, H-10), 5.66 (s, 1H, H-7), 5.22 (d, 1H, $J_{\text{OH}-3}$ = 4.8 Hz, OH), 5.01 (d, 1H, $J_{\text{OH}-2}$ = 6.8 Hz, OH), 4.64 (d, 1H, J_{1-2} = 3.6 Hz, H-1), 4.32 (q, 2H, J_{13-14} = 6.8 Hz, H-13), 4.18 (dd, 1H, J_{6B-5} = 4.7 Hz, J_{6B-6A} = 10.0 Hz, H-6B), 3.72 (t, 1H, $J_{6A-6B, 6A-5}$ = 10 Hz, H-6A), 3.56–3.62 (m, 2H, H-3, H-5), 3.33–3.43 (m, 2H, H-2, H-4), 3.33 (H_2O), 3.31 (s, 3H, OCH_3), 1.32 (t, 3H, J = 7.2 Hz, H-14); ^{13}C NMR (100 MHz, DMSO- d_6 , TMS) δ (ppm): 165.4, 142.4, 130.2, 128.9, 126.7, 100.5, 99.9, 81.3, 72.4, 69.8, 68.2, 62.3, 60.8, 54.7, 14.1; TOF-MS, m/z calculated for $\text{C}_{17}\text{H}_{22}\text{O}_8$ 354.1315, found: m/z 354.1330. Compound **7b** (isolated as a white solid in 72% yield, mp 148–150 °C, $[\alpha]_D^{20} +82$ (c 0.48 g/100 mL, MeOH); IR (KBr, cm^{-1}): ν = 3179–3633, 2977, 2858, 1728, 1369, 1273, 1071, 1031, 760; ^1H NMR (400 MHz, CDCl_3 , TMS) δ (ppm): 8.04 (d, 2H, J_{9-10} = 8.4 Hz, H-9), 7.56 (d, 2H, J_{10-9} = 8.4 Hz, H-10), 5.57 (s, 1H, H-7), 4.80 (d, 1H, J_{1-2} = 4.0 Hz, H-1), 4.26–4.32 (m, 3H, H-6B, H-13), 3.93 (t, 1H, J_{3-4} = 9.1 Hz, H-3), 3.72–3.84 (m, 2H, H-5,

H-6A), 3.58–3.66 (m, 1H, H-2), 3.48–3.53 (m, 1H, H-4), 3.46 (s, 3H, OCH_3), 2.86 (s, 1H, OH), 2.36 (d, 1H, $J_{\text{OH}-2}$ = 9.5 Hz, OH), 1.80 (h, 2H, J_{14-15} = 7.2 Hz, H-14), 1.02 (t, 3H, J_{15-14} = 7.4 Hz, H-15); ^{13}C NMR (100 MHz, CDCl_3 , TMS) δ (ppm): 166.3, 141.4, 131.2, 129.6, 126.4, 101.1, 99.7, 80.9, 72.9, 71.8, 68.9, 66.7, 62.3, 55.6, 22.1, 10.5; TOF-MS, m/z calculated for $\text{C}_{18}\text{H}_{24}\text{O}_8$ 368.1471, found: m/z 368.1478. Compound **7c** (isolated as a white solid in 65% yield, mp 146–147 °C, $[\alpha]_D^{20} +72$ (c 0.5 g/100 mL, MeOH); IR (KBr, cm^{-1}): ν = 3133–3006, 2957, 2868, 1723, 1376, 1277, 1088, 1031, 769; ^1H NMR (400 MHz, CDCl_3 , TMS) δ (ppm): 8.03 (d, 2H, J_{9-10} = 8.3 Hz, H-9), 7.56 (d, 2H, J_{10-9} = 8.3 Hz, H-10), 5.56 (d, 1H, J_{1-2} = 4.0 Hz, H-1), 4.28–4.33 (m, 3H, H-13, H-6B), 3.92 (t, 1H, J_{3-4} = 9.4 Hz, H-3), 3.71–3.83 (m, 2H, H-5, H-6A), 3.57–3.65 (m, 1H, H-2), 3.47–3.52 (m, 1H, H-4), 3.45 (s, 3H, OCH_3), 2.96 (s, 1H, OH), 2.44 (d, 1H, $J_{\text{OH}-2}$ = 9.5 Hz), 1.75 (p, 2H, J_{14-15} = 6.7 Hz, H-14), 1.46 (h, 2H, J_{15-16} = 6.7 Hz, H-15), 0.97 (t, 3H, J_{16-15} = 7.4 Hz, H-16); ^{13}C NMR (100 MHz, CDCl_3 , TMS) δ (ppm): 166.3, 141.4, 131.2, 129.6, 126.4, 101.1, 99.8, 72.9, 71.7, 68.9, 65.0, 62.3, 55.6, 30.7, 19.2, 13.7; TOF-MS, m/z calculated for $\text{C}_{19}\text{H}_{26}\text{O}_8$ 382.1628, found: m/z 382.1628. Compound **7d** (isolated as a white solid in 67% yield, mp 138–140 °C, $[\alpha]_D^{20} +58$ (c 0.58 g/100 mL, MeOH); IR (KBr, cm^{-1}): ν = 3119–3600, 2924, 2854, 1717, 1372, 1269, 1084, 1039, 746; ^1H NMR (250 MHz, CDCl_3 , TMS) δ (ppm): 8.03 (d, 2H, J_{9-10} = 8.2 Hz, H-9), 7.56 (d, 2H, J_{10-9} = 8.1 Hz, H-10), 5.56 (s, 1H, H-7), 4.80 (d, 1H, J_{1-2} = 3.8 Hz, H-1), 3.28–4.33 (m, 3H, H-13, H-6B), 3.85–3.96 (m, 1H, H-3), 3.70–3.81 (m, 2H, H-5, H-6A), 3.58–3.66 (m, 1H, H-2), 3.50–3.53 (m, 1H, H-4), 3.45 (s, 3H, OCH_3), 2.89 (s, 1H, OH), 2.39 (d, 1H, $J_{\text{OH}-2}$ = 9.5 Hz, OH), 1.76 (p, 2H, J_{18-19} = 6.9 Hz, H-18), 1.28–1.45 (m, 10H, H-14–17), 0.88 (t, 3H, J_{20-19} = 6.8 Hz, H-20); ^{13}C NMR (62.5 MHz, CDCl_3 , TMS) δ (ppm): 165.9, 142.8, 130.7, 129.4, 127.2, 101.1, 100.4, 81.8, 72.9, 70.3, 68.6, 65.2, 62.7, 55.2, 31.6, 29.04, 29.01, 28.5, 25.8, 22.5, 14.4; TOF-MS, m/z calculated for $\text{C}_{23}\text{H}_{34}\text{O}_8$ 438.2254, found: m/z 438.2284. Compound **7e** (isolated as a white solid in 45% yield, mp 132–134 °C, $[\alpha]_D^{20} +58$ (c 0.37 g/100 mL, MeOH); IR (KBr, cm^{-1}): ν = 3141–3631, 2926, 2852, 1722, 1373, 1272, 1084, 1037, 756; ^1H NMR (400 MHz, DMSO- d_6 , TMS) δ (ppm): 7.94 (d, J_{10-9} = 8.3 Hz, H-10), 7.60 (d, J_{9-10} = 8.3 Hz, H-10), 5.62 (s, 1H, H-7), 4.81 (s, 1H, OH), 4.64 (d, 1H, J_{1-2} = 3.6 Hz, H-1), 4.58 (s, 1H, OH), 4.27 (t, 2H, J_{13-14} = 6.6 Hz, H-13), 4.17 (dd, 1H, J_{6B-5} = 4.7 Hz, J_{6B-6A} = 10 Hz, H-6B), 3.71 (t, 1H, $J_{6A-6B, 6A-5}$ = 10.0 Hz), 3.58–3.65 (m, 2H, H-5, H-3), 3.35–3.43 (m, 2H, H-4, H-2), 3.33 (s, 3H, OCH_3), 1.71 (p, 2H, J_{14-15} = 7.0 Hz, H-14), 1.24–1.39 (m, 27H, H-15–H-27), 0.85 (t, 3H, J_{28-27} = 6.7 Hz, H-28); ^{13}C NMR (100 MHz, DMSO- d_6 , TMS) δ (ppm): 165.5, 142.5, 130.5, 128.8, 126.6, 100.7, 100.1, 81.6, 72.8, 70.1, 68.4, 64.7, 62.5, 54.9, 31.2, 28.5–28.9, 28.2, 25.4, 21.9, 13.7; TOF-MS, m/z calculated for $\text{C}_{31}\text{H}_{50}\text{O}_8$ 550.3506, found: m/z 550.3677.

4.2. Gelation test for compounds

The gelation test was carried out in various organic solvents at 10–150 mmol L^{-1} concentration range in a 2 mL vial. Mixtures were heated near to the solvent boiling point in an oil bath and allowed to cool slowly at room temperature for approximately 1 h. Next, vials were gently agitated, inverted, and classified (Table 1). All solvents used were previously distilled and dried with molecular sieves 4 Å.

4.3. FTIR analyses

FT-IR spectra were acquired in a BOMEM NB spectrophotometer, model 100-E coupled to a WATLON, model 988, thermal system. An amount of 0.5 mL of the solution previously heated was carefully inserted in ZnSe cells, and temperature range was set within 50 and 30 °C. Spectra were acquired with eight scan in the 4000–

600 cm⁻¹ range with a resolution of 4 cm⁻¹. Finally, the spectra were plotted using Origin 8.0 software.

4.4. Morphological study with SEM

SEM images of xerogels were obtained on a JEOL SEM 6360-LV. Samples were micropulverized and a thin layer of graphite was applied prior to imaging. Xerogels were prepared by spontaneous evaporation of gels formed by compounds **4b–e** or **7b–e** in *p*-xylene at room temperature.

4.5. DSC analyses

DSC experiments were performed in a TA instrument, model Q100 V9.9. Samples were placed in sealed aluminum can and the thermograms were recorded during the cooling step (80–30 °C) at 2 °C min⁻¹ rate.

4.6. SAXS analyses

Small angle X-ray scattering experiments were performed using SAXS1 beam line of Brazilian Synchrotron Light Laboratory (LNLS, Campinas, Brazil). The wavelength used was 1.488 Å and sample-detector distance 1.5 m. ACCD type two dimensional position-sensitive gas detector was used in these measurements.

4.7. Polarimetry

Optical rotations were determined in a Perkin–Elmer polarimeter, 9585 model, using 589 nm wavelength, and methanol as solvent at 20 °C.

4.8. Melting point

Melting points were determined in a Fisatom apparatus, 430 D model, using capillary tubes. The measurements were performed in duplicate.

Acknowledgments

This work was supported by CNPq (INOMAT/CNPq/MCT) and FAPESP. Authors are indebted to Jason G. Taylor for insightful discussion and for reviewing the manuscript for its English usage. P.C.M.L.M. gratefully acknowledges Institute of Chemistry/UNICAMP for analytical facilities. M.F.A., V.T.S., and L.V. are grateful to CNPq for fellowships. We also acknowledge the Brazilian Synchrotron Light Laboratory (LNLS, Campinas, Brazil) for the use of SAXS1 beam line.

Supplementary data

Supplementary data associated with this article can be found, in the online version, at <http://dx.doi.org/10.1016/j.carres.2012.03.021>.

References

- (a) Estroff, L. A.; Hamilton, A. D. *Chem. Rev.* **2004**, *104*, 1201–1218; (b) Terech, P.; Weiss, R. G. *Chem. Rev.* **1997**, *97*, 3133–3159.
- Zweep, N.; Hopkinson, A.; Meetsma, A.; Browne, W. R.; Feringa, B. L.; van Esch, J. H. *Langmuir* **2009**, *25*, 8802–8809.
- Weiss, R. G.; Terech, P. *Molecular Gels: Materials with Self-Assembled Fibrillar Networks*; Springer: Dordrecht, The Netherlands, 2005.
- (a) Vemula, P. K.; Li, J.; John, G. J. *Am. Chem. Soc.* **2006**, *128*, 8932–8938; (b) van Bommel, K. J. C.; Stuart, M. C. A.; Feringa, B. L.; van Esch, J. *Org. Biomol. Chem.* **2005**, *3*, 2917–2920; (c) Lim, P. F. C.; Liu, X. Y.; Kang, L.; Ho, P. C. L.; Chan, Y. W.; Chan, S. Y. *Int. J. Pharm.* **2006**, *311*, 157–164.
- Maeda, H. *Chem. Eur. J.* **2008**, *14*, 11274–11282.
- (a) Jung, Y. H.; Amaike, M.; Shinkai, S. *Chem. Commun.* **2000**, 2343–2344; (b) van Bommel, K. J. C. V.; Friggeri, A.; Shinkai, S. *Angew. Chem., Int. Ed.* **2003**, *42*, 980–999; (c) Jung, J. H.; Shinkai, S.; Shimizu, T. *Nano Lett.* **2002**, *2*, 17–20.
- (a) Jadhav, S. R.; Vemula, P. K.; Kumar, R.; Raghavan, S. R.; John, G. *Angew. Chem., Int. Ed.* **2010**, *49*, 7695–7698; (b) Bhattacharya, S.; Krishnan-Ghosh, Y. *Chem. Commun.* **2001**, 185–186.
- Carretti, E.; Dei, L.; Weiss, R. G. *Soft Matter* **2005**, *1*, 17–22.
- van Esch, J. H. *Langmuir* **2009**, *25*, 8392–8394.
- Dastidar, P. *Chem. Soc. Rev.* **2008**, *37*, 2699–2715.
- (a) Jeong, Y.; Hanabusa, K.; Masunaga, H.; Akiba, I.; Miyoshi, K.; Sakurai, S.; Sakurai, K. *Langmuir* **2005**, *21*, 586–594; (b) Estroff, L. A.; Hamilton, A. D. *Angew. Chem., Int. Ed.* **2000**, *39*, 3447–3450.
- (a) Murata, K.; Aoki, M.; Suzuki, T.; Harada, T.; Kawabata, H.; Komori, T.; Ohseto, F.; Ueda, K.; Shinkai, S. *J. Am. Chem. Soc.* **1994**, *116*, 6664–6676; (b) George, M.; Weiss, R. G. *Acc. Chem. Res.* **2006**, *39*, 489–497; (c) Hou, Q.; Wang, S.; Zang, L.; Wang, X.; Jiang, J. *J. Colloid Interface Sci.* **2009**, *338*, 463–467.
- (a) Lescanne, M.; Colin, A.; Mondain-Monval, O.; Fages, F.; Pozzo, J.-L. *Langmuir* **2003**, *19*, 2013–2020; (b) Galindo, F.; Burguete, M. I.; Gavara, R.; Luis, S. V. *J. Photochem. Photobiol. A* **2006**, *178*, 57–61.
- (a) Gronwald, O.; Sakurai, K.; Luboradzki, R.; Kimura, T.; Shinkai, S. *Carbohydr. Res.* **2001**, *331*, 307–318; (b) Gronwald, O.; Snip, E.; Shinkai, S. *Curr. Opin. Colloid Interface Sci.* **2002**, *7*, 148–156; (c) Cui, J.; Zheng, J.; Qiao, W.; Wan, X. *J. Colloid Interface Sci.* **2008**, *326*, 267–274; (d) Gronwald, O.; Shinkai, S. *Chem. Eur. J.* **2001**, *7*, 4328–4334.
- Gronwald, O.; Shinkai, S. *J. Chem. Soc., Perkin Trans. 2* **2001**, 1933–1937.
- Friggeri, A.; Gronwald, O.; van Bommel, K. J. C.; Shinkai, S.; Reinhoudt, D. N. *J. Am. Chem. Soc.* **2002**, *124*, 10754–10758.
- (a) Amanokura, N.; Kanekiyo, Y.; Shinkai, S.; Reinhoudt, D. N. *J. Chem. Soc., Perkin Trans. 2* **1999**, 1995–2000; (b) Jung, J. H.; John, G.; Masuda, M.; Yoshida, K.; Shinkai, S.; Shimizu, T. *Langmuir* **2001**, *17*, 7229–7232; (c) John, G.; Jung, J. H.; Masuda, M.; Shimizu, T. *Langmuir* **2004**, *20*, 2060–2065; (d) Bao, C.; Lu, R.; Jin, M.; Xue, P.; Tan, C.; Zhao, Y.; Liu, G. *Carbohydr. Res.* **2004**, *339*, 1311–1316; (e) Jung, J. H.; Rim, J. A.; Han, W. S.; Lee, S. J.; Lee, Y. J.; Cho, E. J.; Kim, J. S.; Shimizu, Q. J. *T. Org. Biomol. Chem.* **2006**, *4*, 2033–2038; (f) Cui, J.; Liu, A.; Guan, Y.; Zheng, J.; Shen, Z.; Wan, X. *Langmuir* **2010**, *26*, 3615–3622.
- Helferich, B.; Schäfer, W. *Org. Synth.* **1941**, *1*, 364.
- Shao, X. B.; Jiang, X. K.; Wang, X. Z.; Li, Z. T.; Zhu, S. Z. *Tetrahedron* **2003**, *59*, 4881–4889.
- Davis, T. S.; Feil, P. D.; Kubler, D. G.; Wells, D. J. *J. Org. Chem.* **1975**, *40*, 1478–1482.
- Evans, M. E. *Carbohydr. Res.* **1972**, *21*, 473–475.
- Cheuk, S.; Stevens, E. D.; Wang, G. *Carbohydr. Res.* **2009**, *344*, 417–425.
- (a) Bielejewski, M.; Lapinski, A.; Luboradzki, R.; Tritt-Goc, J. *Langmuir* **2009**, *25*, 8274–8279; (b) Roy, S.; Chakraborty, A.; Ghosh, R. *Carbohydr. Res.* **2008**, *343*, 2523–2529; (c) Yoza, K.; Amanokura, N.; Ono, Y.; Akao, T.; Shinmori, H.; Takeuchi, M.; Shinkai, S.; Reinhoudt, D. N. *Chem. Eur. J.* **1999**, *5*, 2722–2729.
- Palui, G.; Simon, F.-X.; Schmutz, M.; Mesini, P. J.; Banerjee, A. *Tetrahedron* **2008**, *64*, 175–185.
- (a) Bhattacharya, S.; Acharya, S. N. *G. Chem. Mater.* **1999**, *11*, 3121–3132; (b) Hirst, A. R.; Smith, D. K.; Feiters, M. C.; Geurts, H. P. *M. Chem. Eur. J.* **2004**, *10*, 5901–5910.
- Zhang, Z.; Yang, M.; Hu, C.; Liu, B.; Hu, M.; Zhang, X.; Wang, W.; Zhou, Y.; Wang, H. *New J. Chem.* **2011**, *35*, 103–110.
- Watake, M.; Nakatani, Y.; Itagaki, H. *J. Phys. Chem. B* **1999**, *103*, 2366–2373.
- (a) Jeong, Y.; Friggeri, A.; Akiba, I.; Masunaga, H.; Sakurai, K.; Sakurai, S.; Okamoto, S.; Inoue, K.; Shinkai, S. *J. Colloid Interface Sci.* **2005**, *283*, 113–122; (b) Terech, P.; Allegraud, J. J.; Garner, C. M. *Langmuir* **1998**, *14*, 3991–3998.
- Terech, P.; Ostuni, E.; Weiss, R. G. *J. Phys. Chem.* **1996**, *100*, 3759–3766.